Published in final edited form as:
Cell Physiol Biochem. 2013 ; 32(5): 1386–1402. doi:10.1159/000356577.

Differential Association of the Na^+/H^+ Exchanger Regulatory Factor (NHERF) Family of Adaptor Proteins with the Raft-and the Non-Raft Brush Border Membrane Fractions of NHE3

Ayesha Sultan[a], **Min Luo**[a,b], **Qin Yu**[a,b], **Brigitte Riederer**[a], **Weiliang Xia**[a,c], **Mingmin Chen**[a], **Simone Lissner**[d], **Johannes E. Gessner**[e], **Mark Donowitz**[f], **C. Chris Yun**[g], **Hugo deJonge**[h], **Georg Lamprecht**[d,i], and **Ursula Seidler**[a]

[a]Dept. of Gastroenterology, Hepatology, and Endocrinology, Hannover Medical School, Hannover Germany [b]Dept. of Gastroenterology, Tongji Hospital, Huazhong University of Science and Technology, Wuhan, China [c]Key Lab of Combined Multiorgan Transplantation, 1st Affiliated Hospital, School of Medicine, Zhejiang University, Hangzhou, China [d]1st Medical Department, University of Tübingen, Tübingen, Germany [e]Dept. of Immunology and Rheumatology, Hannover Medical School, Hannover, Germany [f]Div. of Gastroenterology, Departments of Medicine and Physiology, John Hopkins School of Medicine, Baltimore, USA [g]Div. of Digestive Diseases, Dept. of Medicine, Emory University, Atlanta, USA [h]Dept. of Gastroenterology, Erasmus MC, Rotterdam, the Netherlands [i]Dept. of Gastroenterology and Endocrinology, University of Rostock, Rostock, Germany

Abstract

Background/Aims—Trafficking, brush border membrane (BBM) retention, and signal-specific regulation of the Na^+/H^+ exchanger NHE3 is regulated by the Na^+/H^+ Exchanger Regulatory Factor (NHERF) family of PDZ-adaptor proteins, which enable the formation of multiprotein complexes. It is unclear, however, what determines signal specificity of these NHERFs. Thus, we studied the association of NHE3, NHERF1 (EBP50), NHERF2 (E3KARP), and NHERF3 (PDZK1) with lipid rafts in murine small intestinal BBM.

Methods—Detergent resistant membranes ("lipid rafts") were isolated by floatation of Triton X-incubated small intestinal BBM from a variety of knockout mouse strains in an Optiprep step gradient. Acid-activated NHE3 activity was measured fluorometrically in BCECF-loaded microdissected villi, or by assessment of CO_2/HCO_3^- mediated increase in fluid absorption in perfused jejunal loops of anethetized mice.

Results—NHE3 was found to partially associate with lipid rafts in the native BBM, and NHE3 raft association had an impact on NHE3 transport activity and regulation *in vivo*. NHERF1, 2 and

Ursula Seidler, Dept. of Gastroenterology, Hepatology and Endocrinology, Hannover Medical School, Carl-Neuberg-Straße 1, D-30625 (Germany), Tel. +49-511-532-9427, Fax +49-511-532-8428, Seidler.Ursula@mh-hannover.de.

3 were differentially distributed to rafts and non-rafts, with NHERF2 being most raft-associated and NHERF3 entirely non-raft associated. NHERF2 expression enhanced the localization of NHE3 to membrane rafts. The use of acid sphingomyelinase-deficient mice, which have altered membrane lipid as well as lipid raft composition, allowed us to test the validity of the lipid raft concept *in vivo*.

Conclusions—The differential association of the NHERFs with the raft-associated and the non-raft fraction of NHE3 in the brush border membrane is one component of the differential and signal-specific NHE3 regulation by the different NHERFs.

Keywords

PDZ-domain adaptor proteins; Membrane rafts; Cholesterol; Intestine; Salt absorption; Ezrin

Introduction

Na^+/H^+ exchangers regulate salt and water absorption and maintain systemic pH within the physiological range [1]. NHE3, encoded by *slc9a3* in mice [2, 3], is the major absorptive Na^+/H^+ exchanger in intestinal and renal epithelium [4], where it is expressed in the apical membrane and in recycling endosomes [5]. It is involved in electroneutral Na^+ absorption from the lumen, a mechanism driven by the electrochemical gradient maintained by the activity of the Na^+/K^+-ATPase pump on the basolateral membrane [6, 7]. *Nhe3*$^{-/-}$ mice have an absorptive defect in the intestine and the kidney, mild acidosis, and a shortened lifespan [4].

Post-translational modifications, particularly phosphorylation [8], interactions with cytoskeletal elements [9], and electrostatic interactions of the cationic cytoplasmic tail of NHE3 with polyanionic lipids at the inner leaflet of the plasma membrane [10] alter NHE3 activity. The members of the Na^+/H^+ Exchanger Regulatory Factor (NHERF) family of PDZ-adaptor proteins interact with the C-terminal cytoplasmic domain of transporters and channels such as NHE3, Down *R*egulated in Adenoma (DRA), Putative Anion Transporter1 (PAT1) and Cystic Fibrosis Transmembrane Conductance Regulator (CFTR), and form multi-molecular assemblies with the underlying cytoskeleton and associated proteins, thereby modulating such diverse processes as protein trafficking, membrane retention and the formation of signaling platforms [8, 11–13]. These highly homologous NHERF PDZ-adaptors, though expressed in the same spatiotemporal coordinates of the apical epithelial membrane, are not functionally redundant. They have been shown to differentially regulate NHE3 in response to specific agonists [14–18]. Currently, targeting NHERF-mediated multicomplex formation by small molecules is considered a technically challenging, but highly desirable drug development strategy.

An additional aspect of regulation of apical NHE3 is the membrane lipid environment [10] and the association of NHE3 with cholesterol and sphingolipid-enriched membrane rafts (“lipid rafts”) [19, 20]. Defined biochemically, rafts resist solubilisation in nonionic detergents, enabling them to be separated as detergent resistant membranes (DRMs) by flotation in density gradients [21]. NHE3 has been reported to be partially raft-associated in rabbit ileum [19], and substantially raft-associated in rat renal epithelium [22, 23]. It was

further shown in opossum kidney cells that ~50% NHE3 localized to rafts, and this pool was functionally active, since methyl-β cyclodextrin (MβCD)-mediated disruption of membrane rafts decreased NHE3 activity [20]. Due to their inherent protein-lipid oligomerizing interactions, membrane rafts are believed to enable cosegregation and thus functional interaction of proteins in biological membranes [24]. This function of rafts is similar to that rendered by the NHERFs – the assembly of multimolecular complexes. Both rafts and NHERF-PDZ scaffolds interact structurally with the cytoskeletal elements [6, 25]. In the targeting and localization of NHE3 to brush border membrane (BBM), it is not clear if there is any crosstalk between membrane rafts and NHERF PDZ-adaptors.

In this study, we have addressed the proportions of the NHE3 pool in the native murine small intestinal brush border membrane which associates with raft and non-rafts, respectively, and tested whether this raft association of NHE3 has implications for transport function. We then studied the co-segregation of NHERF1–3 with the raft-associated and the non-raft pools of NHE3 and observed a differential association of the different NHERFs with the raft and the non-raft pools of NHE3.

Material and Methods

Materials

Chemicals were obtained from Sigma-Aldrich and Applichem. 2', 7'-bis (carboxyethyl)-5, 6-carboxyfluorescein (BCECF) was from Invitrogen. Hoe642 was kindly provided by Sanofi-Aventis (Frankfurt, Germany). OptiPrep gradient was from PROGEN Biotechnik (Germany). Rabbit Polyclonal anti-rat NHE3 IgG was used at a dilution of 1:2000 (Alpha Diagnostic). Mouse flotillin2 antibody was used at a dilution of 1:2000 (Santacruz Biotechnologies). Rabbit NHERF1 (Ab5199) and NHERF2 (Ab 2170) antibodies were used at 1:10,000 and 1:5000 dilutions, respectively (Prof. Chris C. Yun, Emory Univ., Atlanta). Rabbit PDZK1/NHERF3 peptide-1 was used at dilutions of 1:2000 (Prof. Hugo deJonge, Erasmus MC, Rotterdam). Rabbit Ezrin antibody was used at a dilution of 1:1000 (Cell Signaling). The anti-rabbit and anti-mouse, HRP-conjugated secondary antibodies were used at a dilution of 1:10,000 (Abcam).

Mice strains

Acid sphingomyelinase (*ASM*)$^{-/-}$ mice were generated at the laboratory of E. Schuchman [26] and congenic on the C57B/6 backround. Genotyping was done by PCR as previously described [26]. *Nherf1*$^{-/-}$ mice were generated in the laboratory of E.J. Weinman as described earlier [27]. *Nherf2*$^{-/-}$ mice were originally generated from Lexicon genetics clone OST2298 [28]. *Nherf3*$^{-/-}$ mice were originally generated in the laboratory of O. Kocher [29]. All NHERF mice were congenic on the FVB/N background to ensure identical background for all NHERF deficient strains. *Nhe3*$^{-/-}$ mice were originally generated in the lab of Gary Shull [4], and bred on both a congenic FVB/N and C57B/6 background. *Dra*$^{-/-}$ mice were originally bred in the laboratory of C. Schweinfest [30] and maintained as described in [31]. PAT1 mice were generated as described in [32] and maintained as described in [31]. Age and sex-matched wild type mice were used as controls. The animals were provided with standardized light and climate conditions with access to chow and water

ad libitum. Animal experiments followed approved protocols of the Hannover Medical School and the local authorities for the regulation of animal welfare.

Preparation of isolated intestinal villi for fluorometry

For measuring pH_i in isolated jejunal villi, the proximal jejunum (approximately 6cm distal to the pylorus) was removed and immediately placed in ice-cold Ringer solution, solution composition in mM:147 NaCl, 4 KCl, 2.2 $CaCl_2$ in 500 μM DTT to prevent mucus clogging of the villi, pH 7.4 as previously described [33].

Fluorometric pH_i measurements in intact villi

For the assessment of acid-activated NHE3 activity in intact microdissected jejunal villi, the technique was used as described by Chen et al. [18, 33] with minor modifications. Villous enterocytes were acidified to pH_i ~6.4 by a brief incubation with a buffer in which 40 mM NaCl was replaced by 40 mM NH_4Cl for 5 min, followed by a buffer in which all Na^+ was replaced by TMA. Acid-activated Na^+/H^+ exchange activity was assessed as the initial rate of pH recovery after the Na^+-free buffer was switched to Na^+-containing buffer C (25 NaCl, 95 TMACl, 10 Hepes, 5 Tris, 2.25 KH_2PO_4, 1.5 K_2HPO_4, 1.2 $MgSO_4$, 1.2 Ca-gluconate, 10 glucose, pH 7.4 gassed with oxygen): 50 μM HOE642 was present both in Na^+-free buffer and Na^+-containing buffer C in the first recovery pulse to eliminate the contribution of NHE1 and NHE2: both 50 μM HOE642 and 10 μM S1611 (NHE3 specific inhibitor) were present during the recovery from a second ammonium prepulse to inhibit also NHE3 activity. Emission intensity ratio into pH calibration was performed as described in [34]. The rates of pHi change measured in the experiments were converted to proton flux (J_H^+) by using the equation $J_H^+ = \Delta pH/\Delta t \times \beta i$, where t equals time. NHE3 activity was calculated as the proton flux in the first recovery pulse minus the proton flux in the second recovery pulse.

In vivo measurement of fluid absorption in jejunum

The mice were anesthetized by spontaneous inhalation of isoflurane (Forene: Abbott Germany: Wiesbaden, Germany) via a mask, a catheter was placed in the left carotid artery for continuous infusion of (in mM) 200 Na^+, 100 CO_3^{2-}, 5 K^+ and 5 Cl^- at a rate of 0.3ml/h in $ASM^{+/+}$ and $ASM^{-/-}$ mice, to maintain the systemic acid-base and fluid balance. The procedure for measuring jejunal fluid absorption has been previously described in detail [18, 33]. The fluid absorption rates are represented in microliters per centimeter jejunum length per hour ($\mu l \cdot cm^{-1} \cdot h^{-1}$).

Intestinal Brush Border Membrane (BBM) Isolation

The lumen of the small intestine was washed with ice-cold PBS and all the subsequent processes done at 4°C. Intestinal segments were cut open longitudinally and mucosa was harvested by scraping with a glass slide and homogenized in 3ml of buffer A (270 mM mannitol, 12 mM Tris, 16 mM HEPES, 1mM EGTA, 1.006 mM $CaCl_2$, pH 7.4, 40 μg/ml PMSF, 20 μg/ml leupeptin, 20 μg/ml pepstatin A, 20 μg/ml antipain, 1mM DTT, 4 mM benzamidin) and homogenized 3 times for 10 secs by means of an Ultra-Turrax homogenizer (IKA) set at speed 4, with 10 sec intervals on ice. The homogenate was treated by 20 up and down strokes at 1000rpm with a glass on glass potter Potter S (Braun Biotech

International). The process of homogenizing was repeated at 5 min interval on ice. The homogenate was centrifuged at 2000g, for 10min. Supernatant was collected, samples were taken for homogenate analysis, and 1M $MgCl_2$ was added to a final concentration of 10mM with 20 min of mixing and centrifugation at 3000g for 15 min. Supernatant was centrifuged at 30,000g for 30 min. The pellet was homogenized and suspended in buffer B (270 mM Mannitol, 12 mM Tris, 16 mM HEPES, pH 7.4, 40 μg/ml PMSF, 20 μg/ml leupeptin, 20 μg/ml pepstatin A, 20 μg/ml antipain, 1mM DTT, 4 mM benzamidin). 1M $MgCl_2$ precipitation and centrifugation at 3000g for 15 min was repeated. The supernatant was centrifuged at 30,000g for 30 min. The pellet was resuspended in TN buffer (50 mM Tris-Cl, 150 mM NaCl, pH 7.4, 40 μg/ml PMSF, 20 μg/ml leupeptin, 20 μg/ml pepstatin A, 20 μg/ml antipain, 1mM DTT, 4 mM benzamidin) using a 25G needle. This highly enriched BBM fraction was was used without freezing for isolation of DRMs. A small amount of BBM was stored at −80°C for running as a control on PAGE.

Detergent resistant membrane isolation

For isolating lipid rafts, 1mg of the BBM was treated with Triton-X-100, final concentration 1%, in TN buffer, up to a volume of 1ml for 30 min with gentle mixing on an orbital rotator. The sample was adjusted to 40% by using 2ml of 60% OptiPrep (Axis-Shield, PROGEN Biotechnik, Heidelberg). A step gradient was generated by using the 3ml of 40% OptiPrep as the lowermost step and steps of decreasing concentrations of OptiPrep- 3.5ml of 35%, 2.5 ml of 25% and 2ml of 15% OptiPrep/TN buffer were overlaid. Centrifugation was carried out in a SW-41 Ti Beckman Coulter rotor at 170,000g, for 4h. 1 ml fractions were collected from the top and precipitated with 2 volumes of ice-cold acetone, stored at −20°C overnight. The precipitated protein pellets were re-suspended in 100 μl SDS-PAGE sample buffer at 65°C for 15 min and equal volumes of each fraction analyzed by PAGE followed by western blotting.

Immunoblot analysis

Protein samples were resolved on 10% SDS-PAGE, transferred to PVDF membrane (GE Healthcare Life Sciences). Blots were blocked and first incubated with primary antibodies overnight at 4°C followed by respective HRP conjugated secondary antibodies for 1hr at room temperature. Blots were developed by using ECL (GE Healthcare Life Sciences) and signals quantitated by ImageJ software for gel analysis.

Immunohistochemical analysis of NHE3 distribution along the terminal web-microvillar axis

To determine the distribution of NHE3 along the terminal web-microvillar axis of the small intestinal BBM of $ASM^{-/-}$ and $ASM^{+/+}$ mice, we performed immunohistochemical staining of NHE3 and f-actin and analysed the distribution as previously described [18, 35]. The localisation of the NHE3 as compared to f-actin (terminal web) was assessed by ImageJ software as has been previously described in detail [18]. The peak value of f-actin profile was taken as reference for plotting the NHE3 profile. For each condition a minimum of fifteen cells were taken into consideration from each image. The graph shows the mean of the intensity profiles.

Statistical analyses

Values are expressed as mean ± SEM, with the number of experiments (mice or WT and KO pairs) given in parenthesis. Statistical comparisons were either made using a 2-tailed, unpaired Student's *t* test for single-value comparisons or by ANOVA with *post hoc* analysis for multiple comparisons. Data was considered significant when the *p* value was less that 0.05.

Results

Antibody specificity

Figure 1A demonstrates the specificity of anti-NHE3 and anti-NHERF2 and anti- NHERF3 antibodies to detect the respective proteins in the murine small intestinal brush border membrane (BBM). As shown previously, there is cross-reactivity of the NHERF2 antibody for NHERF1 (Fig. 1A), but the different size distributions and signal intensities of the proteins allow the separation of the bands by Western analysis (though not by immunohistochemistry). Figure 1B shows BBM (different preparations from those utilized in Figure 1A) from NHERF1 KO, NHERF2 KO and WT small intestine, each probed both with the anti-NHERF1 antibody, as well as with the anti-NHERF2 antibody. The gel was an extra long one, 8% instead of 10% polyacrylamide, designed to separate proteins with little difference in size. The anti-NHERF1 antibody stains three bands, all of which are absent in the absence of NHERF1 expression and present in the absence of NHERF2 expression. The anti-NHERF2 antibody stains 4 bands, two of which are absent in the NHERF1 KO BBM but present in NHERF2 KO BBM, and therefore represent the cross reactivity of the NHERF2 antibody with NHERF1 protein. The uppermost band of NHERF1 seen with the anti-NHERF1 antibody is not visualized with the anti-NHERF2 antibody, but is likely NHERF1, because it is absent in the NHERF1 KO BBM.

NHERF PDZ-adaptors are strongly enriched in the small intestinal brush border

Figure 2 demonstrates the enrichment of NHE3 as well as its interaction partners, ezrin and NHERF1–3, in the BBM as compared to the homogenate (HG). The divalent cation BBM isolation procedure is not specifically limited to isolating integral membrane proteins, but also results in the isolation of a significant amount of strongly BBM associated proteins such as the cytoskeleton associated proteins ezrin and the sub-apical scaffold forming NHERF-PDZ adaptors, NHERF1, 2 and 3. NHERF1 and NHERF2 were found almost exclusively in the BBM, while NHERF3 as well as ezrin was also present in the homogenate in substantial amounts (Fig. 2). In relation to NHERF-1 and NHERF-3, the signal for NHERF-2 is weak at the same exposure time of the blot membrane, which reflects the relatively low NHERF-2 expression in relation to NHERF1 and NHERF3 in the murine small intestine [17]. Figure 2 shows the strong association between membrane proteins (i.e. NHE3) and membrane associated proteins such as ezrin and the NHERFs. In contrast, the early endosomal marker Rab5 was predominantly found in endosomal and trafficking pools in the homogenate.

NHE3 partially associates with rafts in the BBM

DRM isolation from enriched BBM of small intestine from WT mice indicated two distinct membrane populations of NHE3 on the basis of distribution of the lipid raft marker flotillin2. Flotillin2 was found only in fractions 3–5 which are designated as rafts on the basis of OptiPrep densities (25% to 25%–35% interface) (Fig. 3A). Western blot analysis demonstrates that, while the majority of NHE3 is non-raft associated, there is a population of total BBM NHE3 protein (~20%), which associates with membrane rafts (Fig. 3B).

Differential distribution of NHERF1, 2 and 3 with the lipid raft and the non-raft BBM pool

We next investigated the distribution of individual NHERF PDZ-adaptors proteins in DRMs from WT enterocyte BBM. We found a differential association of individual NHERF proteins with rafts and non-rafts (Fig. 3A,B). While NHERF1 associates to a small degree, and NHERF2 to a high degree with lipid rafts, NHERF3 is excluded from rafts and entirely found in the non-rafts (Fig. 3A,B). Both for NHERF1 as well as for NHERF2, it appears that the upper (larger) of the two bands detected by antibodies for each NHERF is enriched in the lipid raft fraction. We do not currently know why we see multiple bands with very similar size for the NHERFs, the most likely explanations are lipid modifications, protein phosphorylation and other posttranslational modifications.

NHE3 and NHERF raft association in the BBM of mice deficient for NHERF1–3

Given the ability of the NHERFs to interact with NHE3, with each other, as well as with other NHE3 “signalosome” interaction partners, our next question was if the expression of NHERF1–3 influences the raft and non-raft association of NHE3, or of each other. We therefore studied NHE3 raft association in the small intestine of mice lacking NHERF1, NHERF2 or NHERF3. Compared to WT, in NHERF1 KO enterocyte BBM, raft-association was higher for NHE3 (34%±9.1) and for NHERF2 (51%±4.4) (Fig. 3 C,D). NHERF3 was again non-raft associated, identical to the situation in WT (Fig. 3 C,D).

In NHERF2 KO enterocyte BBM, we observed a reduction of NHE3 localisation to rafts. NHERF1 and NHERF3 associations were unaltered (Fig. 3 E,F). The marked decrease of NHE3 in raft microdomains suggests that NHERF2 is involved in targeting and/or retention of NHE3 in rafts. Thus, among the NHERFs, NHERF2 emerges as the potential NHERF candidate modulating the transport activity of the lipid raft-associated NHE3 population. NHERF3 KO BBM showed a higher percentage of NHERF1 and NHERF2 in rafts (Fig. 3 G,H), but not of NHE3.

These data indicate that the NHERF PDZ-adaptors, possibly due to their binding to NHE3 as well as to each other, are involved in regulating the localization of NHE3 and of each other to different membrane microdomains.

Raft association of NHE3 in DRA KO and PAT-1 BBM

The established functional interaction partner of NHE3 is the anion exchanger DRA (Slc26a3), which has been demonstrated to be important for small intestinal Cl^- absorption [36, 37]. Like NHE3, DRA has a PDZ binding motif and binds to NHERF-2 and NHERF-3 [38, 39], has been shown to be raft-associated [40], and has been proposed to cluster with

NHE3 during salt absorption [38, 12]. We therefore asked the question whether DRA may function as an assembly protein for NHE3 into the rafts. However, the distribution of NHE3 (Fig. 3A,B), as well as the NHERFs (data not shown) into raft and non-raft fractions was not significantly altered in the BBM of DRA KO small intestine (Fig. 4A,B). Another interaction partner of NHE3, less well established, is the Slc26 family member PAT-1 (Slc26a6) [41], but its absence also did not significantly influence NHE3 raft association (data not shown).

Ezrin association with rafts

Ezrin, known to bind both to NHERF1 and NHERF2 via their ERM domain, as well as directly to NHE3 [see 8, 11, for review], was found to strongly cosegregate with NHE3 and NHERF2 into the same raft fraction, but was also present in the non-raft BBM fraction (Fig. 4 C,D).

Raft-associated NHE3 in the murine small intestinal BBM is functionally active

Similar to NHE3 in the BB of opossum kidney cells [20], a decrease in acid-activated NHE3 activity of the enterocytes within micro-dissected jejunual villi was observed upon depletion of cholesterol from the apical membrane by MβCD perfusion (Fig. 5). Cholesterol depletion in cells via MβCD may have additional effects on transport proteins (i.e. reorganization of cellular actin cytoskeleton reducing lateral mobility of both raft and non-raft proteins at the cell surface [42, 43], depolarization of plasma membrane and non-specific depletion of intracellular Ca^{2+} stores [44]. Therefore we sought another means of altering raft lipids. The enzyme acid sphingomyelinase (ASM) hydrolyzes sphingomyelin to ceramide [45]. In ASM-deficient mice, plasma membranes have a higher sphingomyelin/ceramide ratio, as well as ganglioside content compared to those in wild type counterparts [46]. This change in lipid metabolism also affects the DRM lipid composition [47, 48]. We therefore assessed the association of NHE3 with DRMs in ASM KO jejunal BBM. In WT jejunum (C57BL/6 background), a significant fraction of BBM NHE3 associated with membrane rafts (Fig. 6A,B), similar to the results from WT FVB/N jejunum. Interestingly, in ASM KO mice, a shift of both flotillin2 and NHE3 towards even lighter density fractions was observed (Fig. 6A). There was a concomitant increase in overall NHE3 (41.8%±2) association with the raft fractions (Fig. 6B). The fraction of ezrin in the rafts did not appear to be altered (26,1% in WT vs 28% in KO), but the numbers of raft preparation tested for ezrin distribution were too low for statistical evaluation.

To study the functional consequences of a change in membrane lipid composition and a higher percentage of NHE3 in membrane rafts, we measured jejunal basal, acid-activated (by luminal CO_2/HCO_3^- perfusion), and forskolin-inhibited fluid absorptive rates *in vivo*. Basal fluid absorptive rate was significantly higher in ASM KO (131±9.5 $\mu l \cdot cm^{-1} \cdot h^{-1}$) compared to WT jejunum (106±7.4 $\mu l \cdot cm^{-1} \cdot h^{-1}$),$p<0.05$. Upon subsequent intracellular acidification of the jejunal enterocytes by perfusing the lumen with CO_2/HCO_3^-, pH 7.4, a similar increase in NHE3 activity was observed, both in WT (186±10.4, 35.6% increase from basal) and ASM KO jejunum (234±18.4, 34.9% increase from basal) (Fig. 7, left and middle bars). Treatment by 10 μM forskolin resulted in a significant decrease in NHE3 activity in WT mice, but not in ASM KO mice (Fig. 7, right bars).

The localization of NHE3 along the microvillar axis in the BBM was not altered in ASM KO jejunum, as indicated by a similar distribution of the relative NHE3-mediated pixel intensity perpendicular to the terminal web-microvillar axis in relation to F-actin (Fig. 8A), and neither the steady-state pH_i, (Fig. 8B), nor the maximal NHE3 transport rate after ammonium-prepulse-induced intracellular acidification (Fig. 8C), which assesses the total activatable NHE3 pool, was different in microdissected jejunal ASM-deficient and WT villi.

Discussion

Our data suggest that native murine small intestinal enterocytes have two distinct pools of NHE3 in the BBM, a lipid raft-associated and a non-raft-associated pool. This is in accordance with earlier findings in rabbit ileum [19]. The different NHERF adaptor proteins (NHERF1–3) were found to differentially co-segregate with the raft and non-raft fraction of NHE3 in the BBM. NHERF2 was strongly associated with lipid rafts in the BBM, whereas NHERF1 and NHERF3 were not. The data also suggested that the presence of the NHERFs influence the raft association of NHE3, as well as of each other. In a mouse model with a genetic alteration of membrane lipid composition, a higher percentage of NHE3 in the lipid rafts in small intestinal BBM was associated with a higher basal fluid absorptive rate and with less sensitivity to inhibition by FSK. Thus, one reason for the different regulatory functions of this highly homologous family of proteins may be mediated via their association with different pools of NHE3.

The molecular identification of the NHERF proteins as regulators of NHE3 transport function occurred during the search for NHE3 binding proteins that were required for PKA-mediated inhibition of NHE3 transport activity [see 8, 11 for review]. In PS120 fibroblasts, either NHERF1, or NHERF2, was required but sufficient to form a complex between NHE3 and the PKA anchor protein ezrin, bringing PKA into close proximity to NHE3 (hypothetized to be then phosphorylated and thus inhibited) [49]. However, when NHE3 regulation was first studied in the native intestine and the proximal tubule of NHERF1–3-deficient mice, the lack of each NHERF resulted in a specific loss of a subset of regulatory aspects of NHE3 regulation and/or of membrane retention in a signal- and segment specific manner, despite the fact that all three NHERFs were expressed in both enterocytes and in proximal tubule epithelium [14–18]. In murine intestine, the loss of NHERF3, but not of NHERF1 or NHERF2, resulted in a decrease in acid-activated NHE3 activity as well as of cAMP-mediated NHE3 inhibition [15–18]. Although a multitude of additional NHE3 interacting proteins have been identified in the meantime, it is still unclear what determines the specific interaction of one member of the NHERF family, and not the other, with NHE3 in a given signaling event. One explanation would be that NHE3 exists in different pools within the brush border membrane, and these pools are differentially targeted by the different NHERFs.

Associations of membrane proteins within membrane rafts (lipid rafts) is another mode of assembly of membrane proteins [21, 24, 50]. In rat proximal tubule, NHE3 and the Na^+ phosphate co-transporter NaPiII, which both bind to and are regulated by NHERF1, associate with different membrane microdomains [22, 23]. NHE3 was predominantly lipid raft-associated, whereas NaPiII was non-raft associated, and NHERF1 was found only in the

non-raft fraction during angiotensin II-mediated inhibition of sodium and phosphate absorption [23]. In the rabbit ileum, NHE3 was found to associate with lipid rafts to a lesser degree than in rat kidney [19], this paper, suggesting that in the intestinal BBM, at least two NHE3 pools exist – a small raft and a larger non-raft pool.

We hypothesized that the different NHERFs, which all mediate NHE3 inhibition, but do so in response to different agonists or in different cell types, may differentially associate with the raft and the non-raft pool of NHE3 in the murine small intestinal brush border membrane. This was indeed the case, although not in the way we expected. We had assumed that the fact that NHERF1 was shown to be important in cAMP-mediated inhibition of renal but not intestinal NHE3 [14, 15], whereas NHERF3 (PDZK1) was required for intestinal NHE3 inhibition [16, 17], may be due to NHERF1 and NHERF3 interacting with different NHE3 pools, NHERF1 with a non-raft associated pool of NHE3 (in analogy with the kidney) and NHERF3 with a lipid raft-associated pool of NHE3. Instead, we found NHERF2 to be highly raft-associated, NHERF1 only weakly, and NHERF3 to be entirely non-raft associated.

This finding may explain why, in the murine intestine, certain signaling pathways are exclusively NHERF2-dependent, yet only affect a fraction of NHE3 function. For example, the acute stimulation of NHE3 by lysophosphatidic acid [35], and the acute inhibition of NHE3 by heat-stable Eschericia coli enterotoxin, as well as by carbachol [18], only affected a fraction of total acid-activated NHE3 function [18, 35]. One of several potential explanations may be that these signaling pathways, because of their NHERF2 dependency, preferentially or exclusively target the raft-associated pool of NHE3 in the plasma membrane. Of course, many future experiments are necessary to understand the dynamics of NHE3 and NHERF2 into and from the membrane rafts of native intestinal BBM.

We next addressed the question whether the segregation of NHE3 to lipid rafts may be influenced by the NHERFs. While the NHERFs are not integral membrane proteins and would not be able to integrate into the membrane portion of the raft, they may either bind to other raft-associated proteins and thus tether NHE3 to the rafts, or they may target to rafts because of lipid modifications. One such scenario has been found during the study of the cAMP-induced inhibition of the T-cell response, where ezrin brings PKA into proximity with its downstream substrate Csk in lipid rafts by forming a multiprotein complex consisting of PKA-Ezrin-NHERF1-Csk, via the Csk-binding protein/phosphoprotein associated with glycosphingolipid-enriched microdomains (PAG) [51–53]. Therefore we investigated the raft association of NHE3 in BBM isolated from NHERF1–3 deficient mice. The striking finding was a decrease in the raft-associated NHE3 pool in the absence of NHERF2 expression, while it was preserved in the absence of NHERF1 or NHERF3. The absence of NHE3 expression, on the other hand, did not influence the differential association of the NHERFs to the raft and non-raft fraction in the BBM (data not shown). The absence of NHERF1 appeared to increase the raft association of both NHE3 and NHERF2, while the absence of NHERF3 increased the raft association of NHERF1 and NHERF2. The explanation may be the NHERFs bind to each other [54, 55], and the high abundance of NHERF1 in the intestine may tether both NHERF2 and NHE3 to a non-raft localization.

We also investigated whether other raft-associated, NHE3- as well as NHERF-2 interacting partners such as Cl^-/ HCO_3^- exchangers Slc26a3 (DRA), and Slc26a6 (PAT1), may tether either NHERF-2 or NHE3, or both, to the rafts, but the absence of either anion exchanger did not influence the raft association with either NHE3 (Fig. 3A,B) or the NHERFs (data not shown). Ezrin, which binds both the NHERF2 as well as to NHE3 [8, 11], was found to cosegregate both with the raft and the non-raft fraction (Fig. 4C,D), and it would be interesting to study raft association in the absence of ezrin, but the ezrin KO mice die early [56]. Thus, future experiments will be necessary to elucidate the molecular basis for the strong raft association of NHERF2. Membrane raft targeting of proteins is often effected through lipid modifications such as palmitoylation [57]. Whether the NHERF-2 itself binds to rafts, or whether a palmitoylated and/or GPI-anchored NHERF-binding protein such as PAG [51–53], or CD371/tetherin [58] has binding affinity to NHERF-2 and may act as the intermediate, needs further study.

The method of isolating DRMs has been implicated in experimentally “creating” large and stable lipid rafts, whereas in the natural state they may be highly dynamic and nanoscale in size [21, 59]. In addition, the cholesterol depletion of the membrane by MβCD treatment is a frequently employed technique to study the functional importance of raft association of a protein, but this method may cause additional alterations in the plasma membrane, such as a reorganization of cellular actin cytoskeleton reducing lateral mobility of both raft and non-raft proteins at the cell surface [42, 43]. MβCD has also been reported to induce depolarization of plasma membrane and non-specific depletion of intracellular Ca^{2+} stores [44], and it may affect membrane curvature or membrane surface charge, thus interfering with NHE3 activity [1, 6, 10]. Therefore we sought for another means of altering raft lipids and studying the effect on NHE3 raft association and possibly, function. The ASM hydrolyzes sphingomyelin to ceramide, and ceramide molecules coalesce to form large ceramide-enriched rafts [45]. We speculated that one way of influencing membrane rafts by a genetic approach would be to study small intestinal brush border membranes of ASM-deficient mice. These mice have higher serum cholesterol and a higher percentage of glycolipids and gangliosides in their plasma membrane, which also causes changes in lipid raft composition [46–48]. We found the lipid rafts from ASM-deficient mice to have a lower buoyant density (as judged by the shift of flotillin2 to lighter density fractions of the optiprep gradient) and we found a higher percentage of BBM NHE3 to be associated with lipid rafts. The mice also had a significantly higher basal and CO_2/HCO_3^- stimulated fluid absorptive rate *in vivo*, which is a function of active NHE3 in the microvillar region [37]. The maximal acid activation of NHE3 by ammonium prepulse *in vitro*, which is expected to activate all membrane resident NHE3, was not significantly different in ASM-deficient compared to WT villi, and neither was the percentage of NHE3 localized to microvilli (as compared to the microvillar cleft/terminal web region, which is the region with maximal F-actin staining) altered in these mice. Interestingly, the inhibition of fluid absorptive rate by forskolin was significant only in WT mice, suggesting that the NHERF-2 and raft-associated pool of NHE3 may not be the one inhibited by an increase in intracellular cAMP levels. This is consistent with previous observations in the NHERF-deficient mice, where the lack of NHERF3 and to some extent NHERF-1, but not of NHERF2 influenced cAMP-mediated NHE3 inhibition in the intestine [15–18]. It is also consistent with work by Murtazina et al

in opossum kidney cells, where NHE3 raft association was not essential for cAMP inhibition of NHE3 [20]. These are the first *in vivo* experiments confirming that changes in membrane lipid composition as well as increased NHE3 raft association may affect NHE3 activity, but the model is clearly too complex to firmly establish the molecular basis for the change in NHE3 raft association as well as increase in NHE3-mediated fluid absorption. Additional modes of NHE3 regulation, such as membrane curvature, surface charge, or altered protein complex assemblies due to changes in lipid modification of proteins, may also affect the regulation of NHE3-mediated fluid absorption in ASM-deficient mice.

In summary, we found that the Na^+/H^+ exchanger isoform NHE3 exists in two pools in the small intestinal brush border membrane, one found in a detergent-resistant ("lipid raft") membrane fraction, and one not raft-associated. Different NHE3-regulatory NHERF proteins differentially associate with the raft and non-raft pools of NHE3, with NHERF2 being most raft-associated and NHERF3 precluded from rafts. Moreover, NHE3 raft-association was decreased in the absence of NHERF2. This suggests that PDZ adaptor proteins are involved in the tethering of NHE3 to lipid rafts, thus enabling the spatial separation of NHE3 into different pools within the intestinal brush border membrane. Because it has been shown that the lipid environment of the surrounding membrane influences NHE3 transport activity [6, 10], it is also possible that the association of NHE3 with lipid rafts may result in functionally different NHE3 membrane pools. The differential association of the different NHERFs with the raft and non-raft pool of NHE3 may allow signaling molecules to selectively target these different pools of NHE3. The molecular mechanisms and functional consequences of different NHE3-NHERF pools in the intestinal brush border membrane need to be further explored. This may, eventually, result in drug development strategies that specifically target pathophysiologically important, NHERF-mediated NHE3 over- or underfunction.

Acknowledgments

This work was supported by DFG grant SFB621-C9, by the Volkswagen Stiftung (both to U.S.) and by a stipend from the PhD program "Molecular Medicine" of the Hannover Biomedical Research School (to A.S.). We thank Regina Engelhardt, Brigitte Rausch, Natascha Cirpka, Silke Thiele and Denise Renner for their help with the animal breeding and genotyping. In particular, we thank Markus Gräler, Molekulares Krebsfoschungszentrum, Charité, for making available to us $ASM^{+/-}$ breeding pairs, and we thank Burkhard Tümmler and Oliver Pabst for acting as cosupervisors in the thesis committee for A.S. We thank Andrew Short for helpful suggestions regarding the presentation of the arguments and the style of the manuscript.

References

1. Alexander RT, Grinstein S. Na^+/H^+ exchangers and the regulation of volume. Acta Physiol (Oxf). 2006; 187:159–167. [PubMed: 16734752]
2. Orlowski J, Grinstein S. Diversity of the mammalian sodium/proton exchanger SLC9 gene family. Pflugers Arch. 2004; 447:549–565. [PubMed: 12845533]
3. Brett CL, Donowitz M, Rao R. Evolutionary origins of eukaryotic sodium/proton exchangers. Am J Physiol Cell Physiol. 2005; 288:C223–C239. [PubMed: 15643048]
4. Schultheis PJ, Clarke LL, Meneton P, Miller ML, Soleimani M, Gawenis LR, Riddle TM, Duffy JJ, Doetschman T, Wang T, Giebisch G, Aronson PS, Lorenz JN, Shull GE. Renal and intestinal absorptive defects in mice lacking the NHE3 Na^+/H^+ exchanger. Nat Genet. 1998; 19:282–285. [PubMed: 9662405]

5. D'Souza S, Garcia Cabado A, Yu F, Teter K, Lukacs G, Skorecki K, Moore HP, Orlowski J, Grinstein S. The epithelial sodium hydrogen antiporter Na^+/H^+ exchanger 3 accumulates and is functional in recycling endosomes. J Biol Chem. 1998; 273:2035–2043. [PubMed: 9442041]
6. Alexander RT, Grinstein S. Tethering, recycling and activation of the epithelial sodium proton exchanger, NHE3. J Exp Biol. 2009; 212:1630–1637. [PubMed: 19448073]
7. Kato A, Romero MF. Regulation of electroneutral NaCl absorption by the small intestine. Annu Rev Physiol. 2011; 73:261–281. [PubMed: 21054167]
8. Donowitz M, Mohan S, Zhu CX, Chen TE, Lin R, Cha B, Zachos NC, Murtazina R, Sarker R, Li X. NHE3 regulatory complexes. J Exp Biol. 2009; 212:1638–1646. [PubMed: 19448074]
9. Alexander RT, Furuya W, Szászi K, Orlowski J, Grinstein S. Rho GTPases dictate the mobility of the Na/H exchanger NHE3 in epithelia: role in apical retention and targeting. Proc Natl Acad Sci USA. 2005; 102:12253–12258. [PubMed: 16103375]
10. Alexander RT, Jaumouillé, Yeung T, Furuya W, Peltekova I, Boucher A, Zasloff M, Orlowski J, Grinstein S. Membrane surface charge dictates the structure and function of the epithelial Na^+/H^+ exchanger. EMBO J. 2011; 30:679–691. [PubMed: 21245831]
11. Lamprecht G, Seidler U. The emerging role of PDZ adapter proteins for regulation of intestinal ion transport. Am J Physiol Gastrointest Liver Physiol. 2006; 291:G766–G777. [PubMed: 16798722]
12. Seidler U, Singh AK, Cinar A, Chen M, Hillesheim J, Hogema B, Riederer B. The role of the NHERF family of PDZ scaffolding proteins in the regulation of salt and water transport. Ann N Y Acad Sci. 2009; 1165:249–260. [PubMed: 19538313]
13. Fanning AS, Anderson JM. PDZ domains: fundamental building blocks in the organization of protein complexes at the plasma membrane. J Clin Invest. 1999; 103:767–772. [PubMed: 10079096]
14. Murtazina R, Kovbasnjuk O, Zachos NC, Li X, Chen Y, Hubbard A, Hogem BM, Steplock D, Seidler U, Hoque KM, Tse CM, De Jonge HR, Weinman EJ, Donowitz M. Tissue specific regulation of sodium/proton exchanger isoform 3 activity in Na^+/H^+ exchanger regulatory factor 1 (NHERF1) null mice. cAMP inhibition is differentially dependent on NHERF1 and exchange protein directly activated by cAMP in ileum versus proximal tubule. J Biol Chem. 2007; 282:25141–25151. [PubMed: 17580307]
15. Broere N, Chen M, Cinar A, Singh AK, Hillesheim J, Riederer B, Lünnemann M, Rottinghaus I, Krabbenhöft A, Engelhardt R, Rausch B, Weinman EJ, Donowitz M, Hubbard A, Kocher O, de Jonge HR, Hogema BM, Seidler U. Defective jejunal and colonic salt absorption and altered Na^+/H^+ exchanger 3 (NHE3) activity in NHE regulatory factor 1 (NHERF1) adaptor protein deficient mice. Pflugers Arch. 2009; 457:1079–1091. [PubMed: 18758809]
16. Cinar A, Chen M, Riederer B, Bachmann O, Wiemann M, Manns M, Kocher O, Seidler U. NHE3 inhibition by cAMP and Ca^{2+} is abolished in PDZ domain protein PDZK1 deficient murine enterocytes. J Physiol (Lond). 2007; 581:1235–1246. [PubMed: 17395628]
17. Hillesheim J, Riederer B, Tuo B, Chen M, Manns M, Biber J, Yun C, Kocher O, Seidler U. Down regulation of small intestinal ion transport in PDZK1 (CAP70/NHERF3) deficient mice. Pflugers Arch. 2007; 454:575–586. [PubMed: 17347851]
18. Chen M, Sultan A, Cinar A, Yeruva S, Riederer B, Singh AK, Li J, Bonhagen J, Chen G, Yun C, Donowitz M, Hogema B, de Jonge H, Seidler U. Loss of PDZ adaptor protein NHERF2 affects membrane localization and cGMP and Ca^{2+} but not cAMP51 dependent regulation of Na^+/H^+ exchanger 3 in murine intestine. J Physiol (Lond). 2010; 588:5049–5063. [PubMed: 20962002]
19. Li X, Galli T, Leu S, Wade JB, Weinman EJ, Leung G, Cheong A, Louvard D, Donowitz M. Na^+-H^+ exchanger 3 (NHE3) is present in lipid rafts in the rabbit ileal brush border: a role for rafts in trafficking and rapid stimulation of NHE3. J Physiol (Lond). 2001; 537:537–552. [PubMed: 11731584]
20. Murtazina R, Kovbasnjuk O, Donowitz M, Li X. Na^+/H^+ exchanger NHE3 activity and trafficking are lipid raft dependent. J Biol Chem. 2006; 281:17845–17855. [PubMed: 16648141]
21. Simons K, Gerl MJ. Revitalizing membrane rafts: new tools and insights. Nat Rev Mol Cell Biol. 2010; 11:688–699. [PubMed: 20861879]
22. Riquier ADM, Lee DH, McDonough AA. Renal NHE3 and NaPi2 partition into distinct membrane domains. Am J Physiol Cell Physiol. 2009; 296:C900–C910. [PubMed: 19158399]

23. Riquier Brison ADM, Leong PKK, Pihakaski Maunsbach K, McDonough AA. Angiotensin II stimulates trafficking of NHE3, NaPi2, and associated proteins into the proximal tubule microvilli. Am J Physiol Renal Physiol. 2010; 298:F177–F186. [PubMed: 19864301]
24. Lingwood D, Simons K. Lipid rafts as a membrane organizing principle. Science. 2010; 327:46–50. [PubMed: 20044567]
25. Chichili GR, Rodgers W. Cytoskeleton membrane interactions in membrane raft structure. Cell Mol Life Sci. 2009; 66:2319–2328. [PubMed: 19370312]
26. Horinouchi K, Erlich S, Perl DP, Ferlinz K, Bisgaier CL, Sandhoff K, Desnick RJ, Stewart CL, Schuchman EH. Acid sphingomyelinase deficient mice: a model of types A and B Niemann Pick disease. Nat Genet. 1995; 10:288–293. [PubMed: 7670466]
27. Shenolikar S, Voltz JW, Minkoff CM, Wade JB, Weinman EJ. Targeted disruption of the mouse NHERF 1 gene promotes internalization of proximal tubule sodiumphosphate cotransporter type IIa and renal phosphate wasting. Proc Natl Acad Sci USA. 2002; 99:11470–11475. [PubMed: 12169661]
28. Broere N, Hillesheim J, Tuo B, Jorna H, Houtsmuller AB, Shenolikar S, Weinman EJ, Donowitz M, Seidler U, de Jonge HR, Hogema BM. Cystic fibrosis transmembrane conductance regulator activation is reduced in the small intestine of Na^+/H^+ exchanger 3 regulatory factor 1 (NHERF 1) but Not NHERF 2 deficient mice. J Biol Chem. 2007; 282:37575–37584. [PubMed: 17947234]
29. Kocher O, Pal R, Roberts M, Cirovic C, Gilchrist A. Targeted disruption of the PDZK1 gene by homologous recombination. Mol Cell Biol. 2003; 23:1175–1180. [PubMed: 12556478]
30. Schweinfest CW, Spyropoulos DD, Henderson KW, Kim JH, Chapman JM, Barone S, Worrell RT, Wang Z, Soleimani M. Slc26a3 (dra) deficient mice display chloride losing diarrhoea, enhanced colonic proliferation, and distinct up regulation of ion transporters in the colon. J Biol Chem. 2006; 281:37962–37971. [PubMed: 17001077]
31. Singh AK, Liu Y, Riederer B, Engelhardt R, Thakur BK, Soleimani M, Seidler U. Molecular transport machinery involved in orchestrating luminal acid-induced duodenal bicarbonate secretion in vivo. J Physiol. 2013; 591:5377–5391. [PubMed: 24018950]
32. Wang Z, Wang T, Petrovic S, Tuo B, Riederer B, Barone S, Lorenz JN, Seidler U, Aronson PS, Soleimani M. Renal and intestinal transport defects in Slc26a6-null mice. Am J Physiol Cell Physiol. 2005; 288:C957–C965. [PubMed: 15574486]
33. Chen M, Singh A, Xiao F, Dringenberg U, Wang J, Engelhardt R, Yeruva S, Rubio Aliaga I, Nässl AM, Kottra G, Daniel H, Seidler U. Gene ablation for PEPT1 in mice abolishes the effects of dipeptides on small intestinal fluid absorption, short circuit current, and intracellular pH. Am J Physiol Gastrointest Liver Physiol. 2010; 299:G265–G274. [PubMed: 20430876]
34. Hegyi P, Rakonczay Z Jr, Gray MA, Argent BE. Measurement of intracellular pH in pancreatic duct cells: a new method for calibrating the fluorescence data. Pancreas. 2004; 28:427–434. [PubMed: 15097861]
35. Lin S, Yeruva S, He P, Singh AK, Zhang H, Chen M, Lamprecht G, de Jonge HR, Tse M, Donowitz M, Hogema BM, Chun J, Seidler U, Yun CC. Lysophosphatidic acid stimulates the intestinal brush border Na^+/H^+ exchanger 3 and fluid absorption via LPA(5) and NHERF2. Gastroenterology. 2010; 138:649–658. [PubMed: 19800338]
36. Walker NM, Simpson JE, Yen PF, Gill RK, Rigsby EV, Brazill JM, Dudeja PK, Schweinfest CW, Clarke LL. Down-regulated in adenoma Cl/HCO3 exchanger couples with Na/H exchanger 3 for NaCl absorption in murine small intestine. Gastroenterology. 2008; 135:1645–1653. [PubMed: 18930060]
37. Xia WL, Yu Q, Riederer B, Singh AK, Engelhardt R, Yeruva S, Song P, Tian DA, Soleimani M, Seidler U. The Distinct Roles of Anion Transporters Slc26a3 (DRA) and Slc26a6 (PAT 1) in Fluid and Electrolyte Absorption in the Murine Small Intestine. Pflügers Arch.
38. Lamprecht G, Heil A, Baisch S, Lin Wu E, Yun CC, Kalbacher H, Gregor M, Seidler U. The down regulated in adenoma (dra) gene product binds to the second PDZ domain of the NHE3 kinase A regulatory protein (E3KARP), potentially linking intestinal Cl /HCO3 exchange to Na^+/H^+ exchange. Biochemistry. 2002; 41:12336–12342. [PubMed: 12369822]
39. Rossmann H, Jacob P, Baisch S, Hassoun R, Meier J, Natour D, Yahya K, Yun C, Biber J, Lackner KJ, Fiehn W, Gregor M, Seidler U, Lamprecht G. The CFTR associated protein CAP70 interacts

with the apical Cl /HCO3 exchanger DRA in rabbit small intestinal mucosa. Biochemistry. 2005; 44:4477–4487. [PubMed: 15766278]

40. Lissner S, Nold L, Hsieh CJ, Turner JR, Gregor M, Graeve L, Lamprecht G. Activity and PI3 kinase dependent trafficking of the intestinal anion exchanger downregulated in adenoma depend on its PDZ interaction and on lipid rafts. Am J Physiol Gastrointest Liver Physiol. 2010; 299:G907–G920. [PubMed: 20634435]
41. Seidler U, Rottinghaus I, Hillesheim J, Chen M, Riederer B, Krabbenhöft A, Engelhardt R, Wiemann M, Wang Z, Barone S, Manns MP, Soleimani M. Sodium and chloride absorptive defects in the small intestine in Slc26a6 null mice. Pflugers Arch. 2008; 455:757–766. [PubMed: 17763866]
42. Kwik J, Boyle S, Fooksman D, Margolis L, Sheetz MP, Edidin M. Membrane cholesterol, lateral mobility, and the phosphatidylinositol 4,5 bisphosphate dependent organization of cell actin. Proc Natl Acad Sci USA. 2003; 100:13964–13969. [PubMed: 14612561]
43. Kenworthy AK. Have we become overly reliant on lipid rafts? Talking Point on the involvement of lipid rafts in T cell activation. EMBO Rep. 2008; 9:531–535. [PubMed: 18516088]
44. Pizzo P, Giurisato E, Tassi M, Benedetti A, Pozzan T, Viola A. Lipid rafts and T cell receptor signaling: a critical re evaluation. Eur J Immunol. 2002; 32:3082–3091. [PubMed: 12385028]
45. Bollinger CR, Teichgräber V, Gulbins E. Ceramide enriched membrane domains. Biochim Biophys Acta. 2005; 1746:284–294. [PubMed: 16226325]
46. Schuchman EH. Acid sphingomyelinase, cell membranes and human disease: lessons from Niemann Pick disease. FEBS Lett. 2010; 584:1895–1900. [PubMed: 19944693]
47. Galvan C, Camoletto PG, Cristofani F, Van Veldhoven PP, Ledesma MD. Anomalous surface distribution of glycosyl phosphatidyl inositol anchored proteins in neurons lacking acid sphingomyelinase. Mol Biol Cell. 2008; 19:509–522. [PubMed: 18032586]
48. Scandroglio F, Venkata JK, Loberto N, Prioni S, Schuchman EH, Chigorno V, Prinetti A, Sonnino S. Lipid content of brain, brain membrane lipid domains, and neurons from acid sphingomyelinase deficient mice. J Neurochem. 2008; 107:329–338. [PubMed: 18673449]
49. Lamprecht G, Weinman EJ, Yun CH. The role of NHERF and E3KARP in the cAMP mediated inhibition of NHE3. J Biol Chem. 1998; 273:29972–29978. [PubMed: 9792717]
50. Dart C. Lipid microdomains and the regulation of ion channel function. J Physiol (Lond). 2010; 588:3169–3178. [PubMed: 20519314]
51. Ruppelt A, Mosenden R, Grönholm M, Aandahl EM, Tobin D, Carlson CR, Abrahamsen H, Herberg FW, Carpén O, Taskén K. Inhibition of T cell activation by cyclic adenosine 5' monophosphate requires lipid raft targeting of protein kinase A type I by the A kinase anchoring protein ezrin. J Immunol. 2007; 179:5159–5168. [PubMed: 17911601]
52. Brdicková N, Brdicka T, Andera L, Spicka J, Angelisová P, Milgram SL, Horejsí V. Interaction between two adapter proteins, PAG and EBP50: a possible link between membrane rafts and actin cytoskeleton. FEBS Lett. 2001; 507:133–136. [PubMed: 11684085]
53. Stokka AJ, Mosenden R, Ruppelt A, Lygren B, Taskén K. The adaptor protein EBP50 is important for localization of the protein kinase A Ezrin complex in T cells and the immunomodulating effect of cAMP. Biochem J. 2010; 425:381–388. [PubMed: 19857202]
54. Lau AG, Hall RA. Oligomerization of NHERF 1 and NHERF 2 PDZ domains: differential regulation by association with receptor carboxyl termini and by phosphorylation. Biochemistry. 2001; 40:8572–8580. [PubMed: 11456497]
55. Gisler SM, Pribanic S, Bacic D, Forrer P, Gantenbein A, Sabourin LA, Tsuji A, Zhao ZS, Manser E, Biber J, Murer H. PDZK1: I. a major scaffolder in brush borders of proximal tubular cells. Kidney Int. 2003; 64:1733–1745. [PubMed: 14531806]
56. Saotome I, Curto M, McClatchy AI. Ezrin is essential for epithelial organization and villus morphogenesis in the developing intestine. Dev Cell. 2004; 6:855–864. [PubMed: 15177033]
57. Aicart Ramos C, Valero RA, Rodriguez Crespo I. Protein palmitoylation and subcellular trafficking. Biochim Biophys Acta. 2011; 1808:2981–2994. [PubMed: 21819967]
58. Rollason R, Korolchuk V, Hamilton C, Jepson M, Banting G. A CD317/tetherin RICH2 complex plays a critical role in the organization of the subapical actin cytoskeleton in polarized epithelial cells. J Cell Biol. 2009; 184:721–736. [PubMed: 19273615]

59. Klotsch E, Schütz GJ. A critical survey of methods to detect plasma membrane rafts. Phil Trans R Soc Lond B Biol Sci.

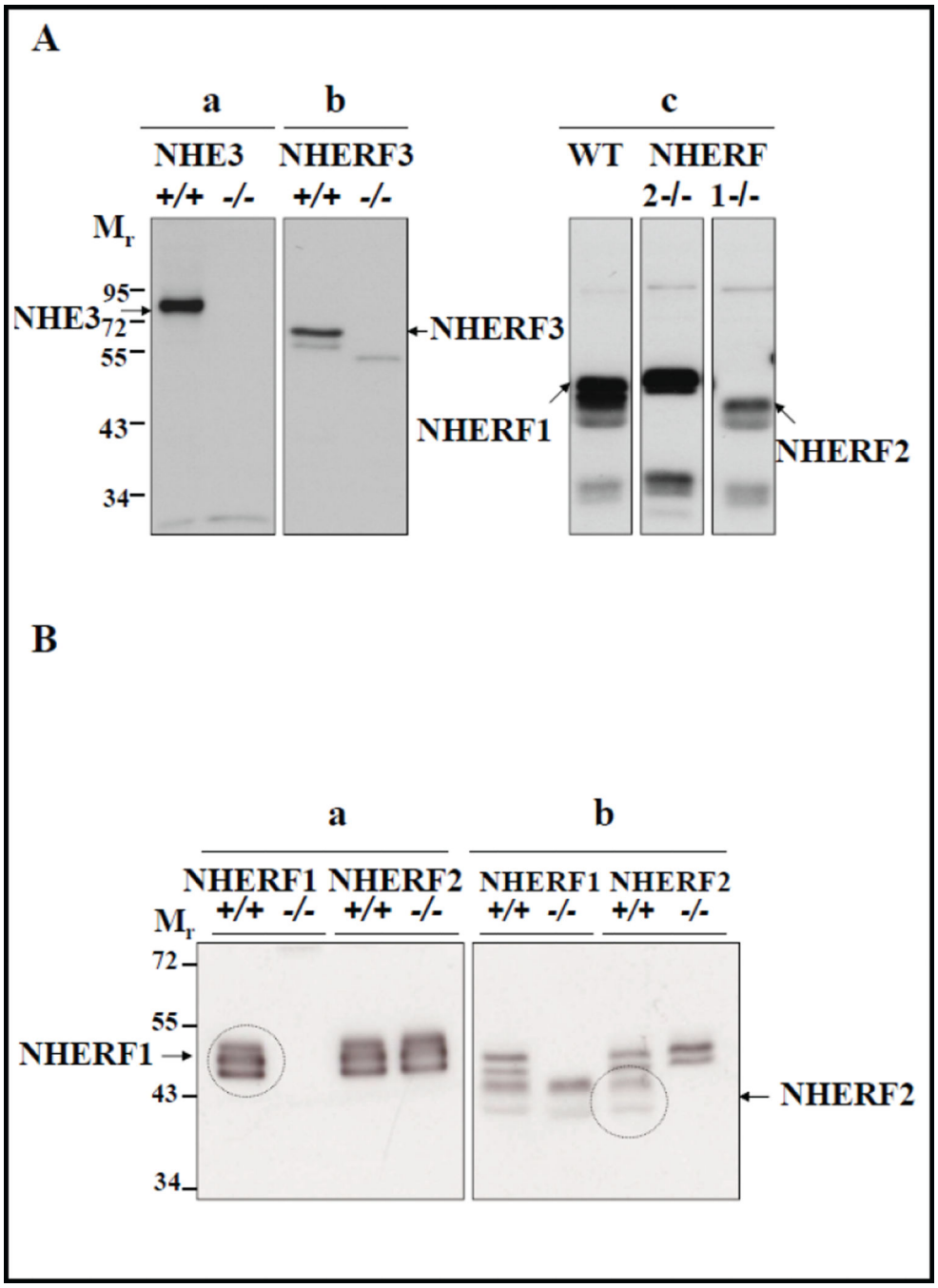

Fig. 1.

Expression of NHE3 and NHERFs in murine BBM. A) Western blots depicting antibody specificities of a) Antibody against NHE3 (~87 KD) in BBM of *Nhe3*$^{+/+}$ and *Nhe3*$^{-/-}$ mice, b) antibody against NHERF3 (~72 KD) in BBM of *Nherf3*$^{+/+}$ and *Nherf3*$^{-/-}$ mice, and c) the rabbit antibody against NHERF2 cross reacts with NHERF1 as depicted by double bands seen at ~48 KD for NHERF1 and ~46 KD for NHERF2 in the WT BBM. The ~46 KD bands were absent in *Nherf2*$^{-/-}$ BBM, and the ~48 KD bands were absent in *Nherf1*$^{-/-}$ BBM. B) This blot displays a different BBM preparation from NHERF1 KO and respective

WT, as well as NHERF2 KO and the respective WT, probed with the anti- NHERF1 antibody (left panel) and the anti-NHERF2 antibody (right panel). Exposure times were 3 seconds (left panel) and 1 minute (right panel). See explanation in text. It is evident that the anti-NHERF1 antibody stains three bands, all of which are absent in NHERF1 KO BBM, and does not cross react with NHERF2. The NHERF2 antibody crossreacts with the lower two bands stained by anti-NHERF1.

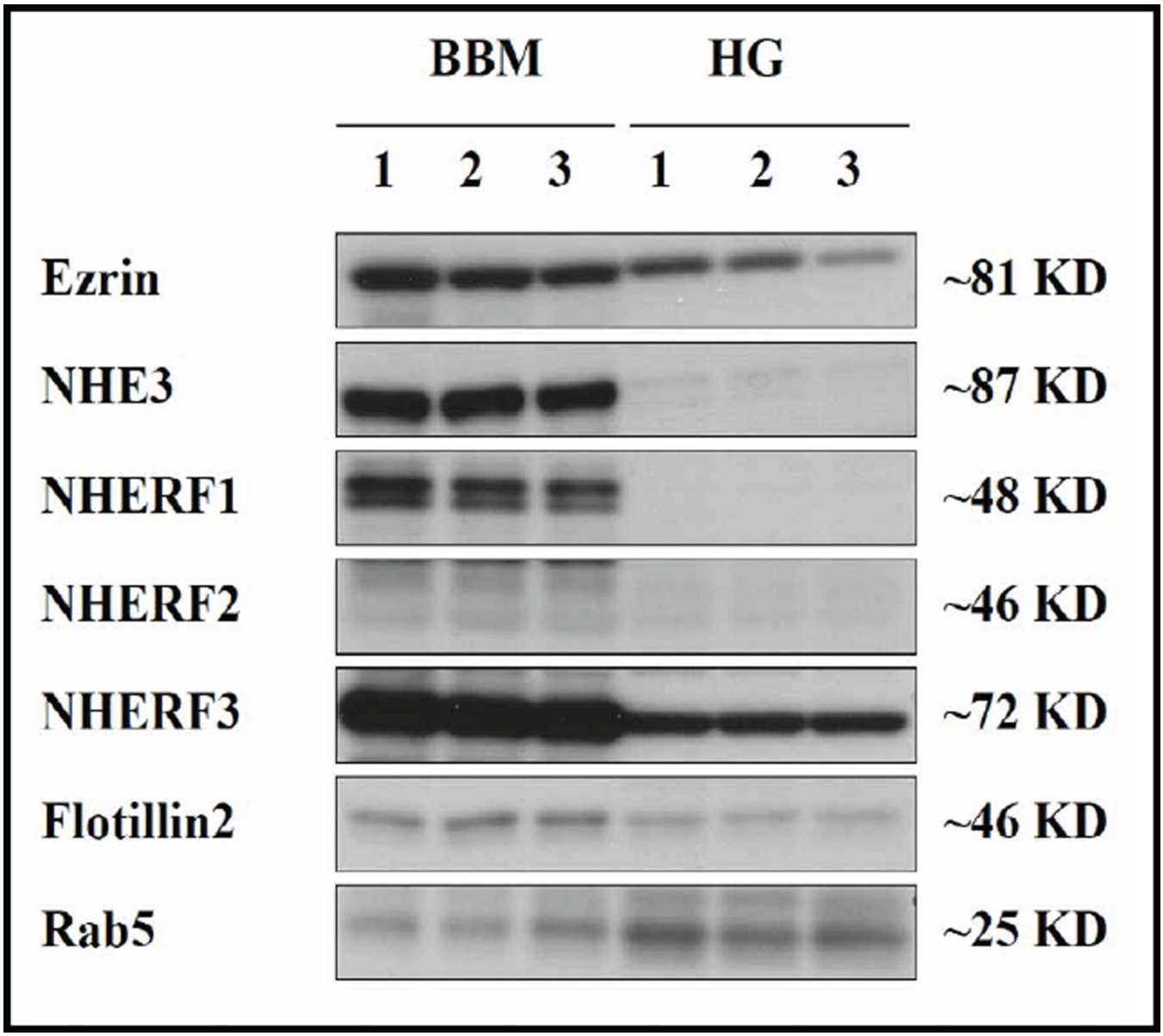

Fig. 2.

Western analysis of brush border membrane association of the proteins under study. Western blots for BBM (left lanes) and cellular homogenate (HG) (right lanes) for ezrin, NHE3, NHERF1, NHERF2, NHERF3, flotillin2 and rab5 (three independent preparations from three mice). NHERF1 and NHERF2, albeit not transmembrane proteins, show a very strong membrane association, ezrin and NHERF3 to a lesser degree, and rab5 not at all.

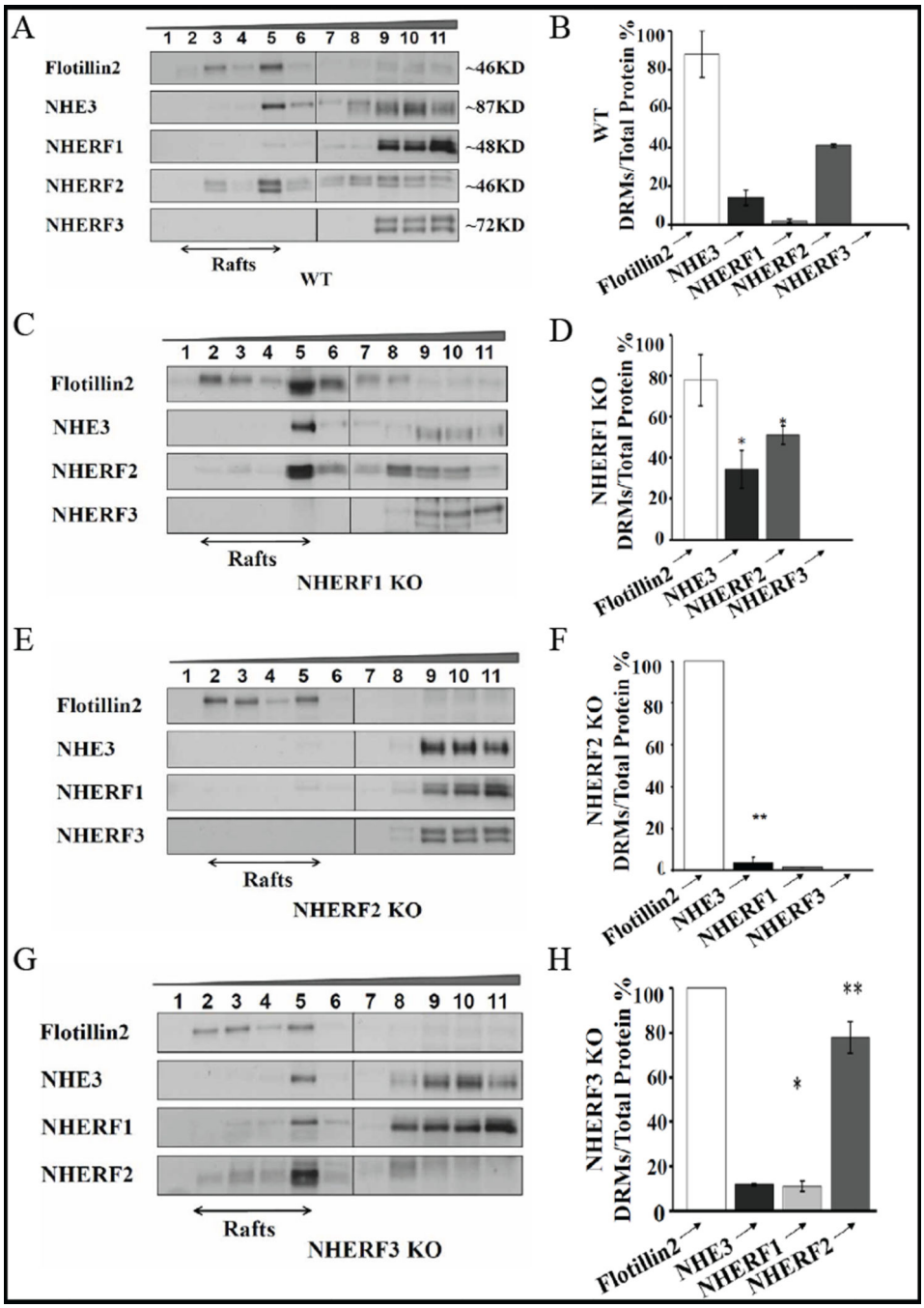

Fig. 3.

NHE3 is partially associated with lipid rafts, and the different NHERFs are differentially associated with the raft and non-raft fraction of BBM. A) NHE3 and the NHERF-PDZ adaptors in rafts and non-rafts of WT mice. Approx. 20% of total BBM NHE3 is found in the raft fractions, which are indicated as fractions 1–5. NHERF1 shows very little raft association, NHERF2 associates strongly with rafts, and NHERF3 is absent from the raft fractions. C), NHERF1 ablation resulted in increased NHE3 and NHERF2 in rafts. E), NHERF2 KO BBM show a decrease in NHE3 in intestinal rafts, demonstrating that NHE3

association with rafts is influenced by the presence of NHERF-2. G) NHERF3 KO BBM show an increase of NHERF1 and NHERF2 raft-association. The Western results correspond to 2–4 independent lipid raft isolations from BBM pooled from 4 mice each. B) Quantification of immune signals from A) NHERF WT BBM showed NHE3 (18%±0.16) and NHERF2 (41%±0.72) in rafts, while NHERF1 raft-association was not significant (2% ±1.03) and NHERF3 not present at all, D) NHERF1 KO showed a significant increase in raft-associated proteins, NHE3 (34.2%±9.1) and NHERF2 (51%±4.4), F) NHERF2 KO showed a strong decrease in NHE3 (3.7%±2.7). H) NHERF3 KO BBM showed an increase of NHERF2 (78%±7.6) and NHERF1 (11%±2.56), but not of NHE3, in the raft fraction. n=2–4, $p>0.05$.

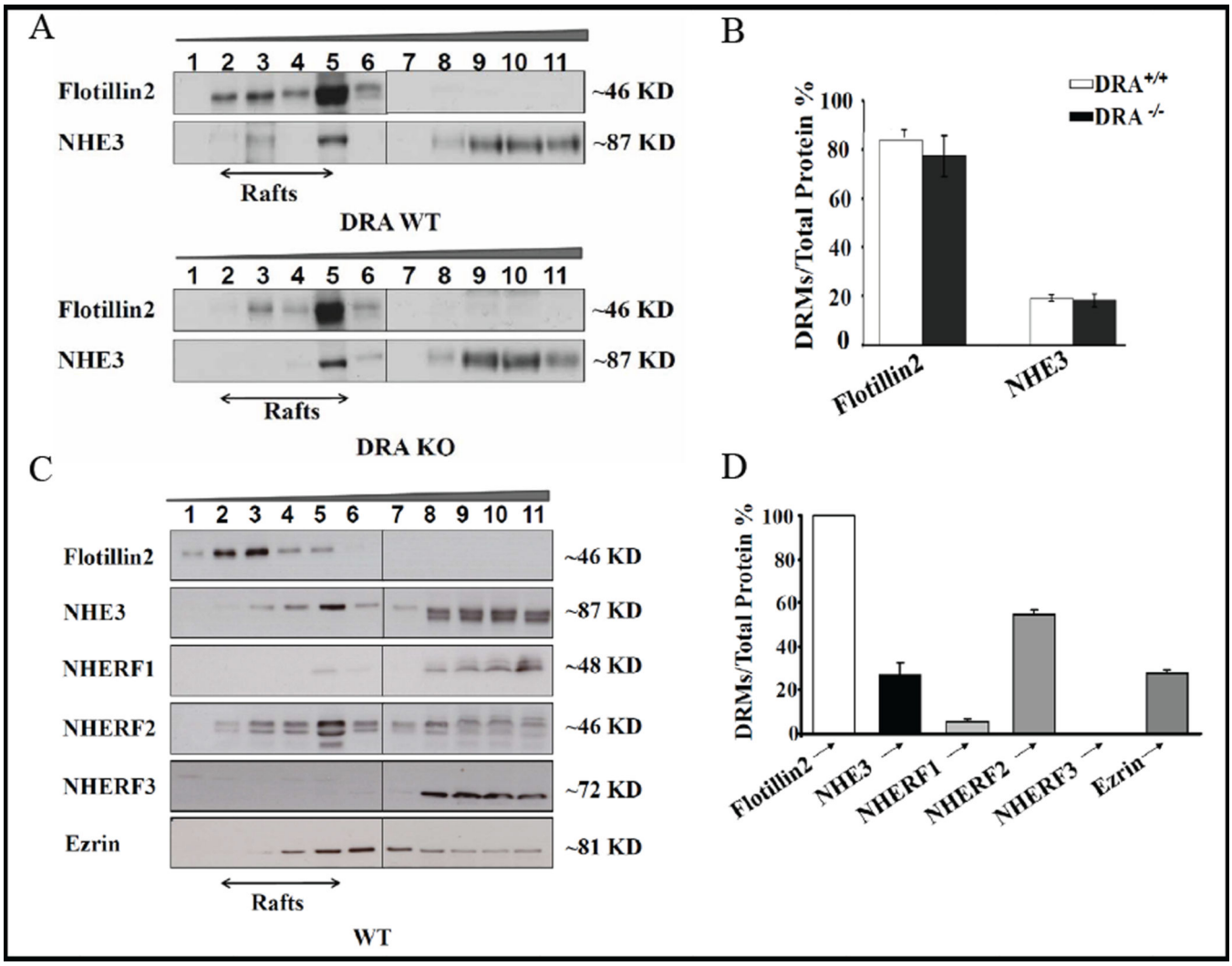

Fig. 4.

NHE3 raft-association is independent of DRA expression and NHE3 cosegregates with ezrin in both the raft and the non-raft fractions. A) Flotillin2 and NHE3 raft-association in BBM of WT and DRA KO mice are similar, implying that NHE3 localizes to rafts independently of its possible physical interaction with DRA. B) Quantitative analysis of immune signals for flotillin2 and NHE3 in WT and DRA KO BBM. n=2–3. C,D) Ezrin (81kD) bands appear in both the raft and the non-raft fraction in C56B/6 WT BBM. A similar distribution was observed in the FVB/N WT BBM (data not shown) n=3.

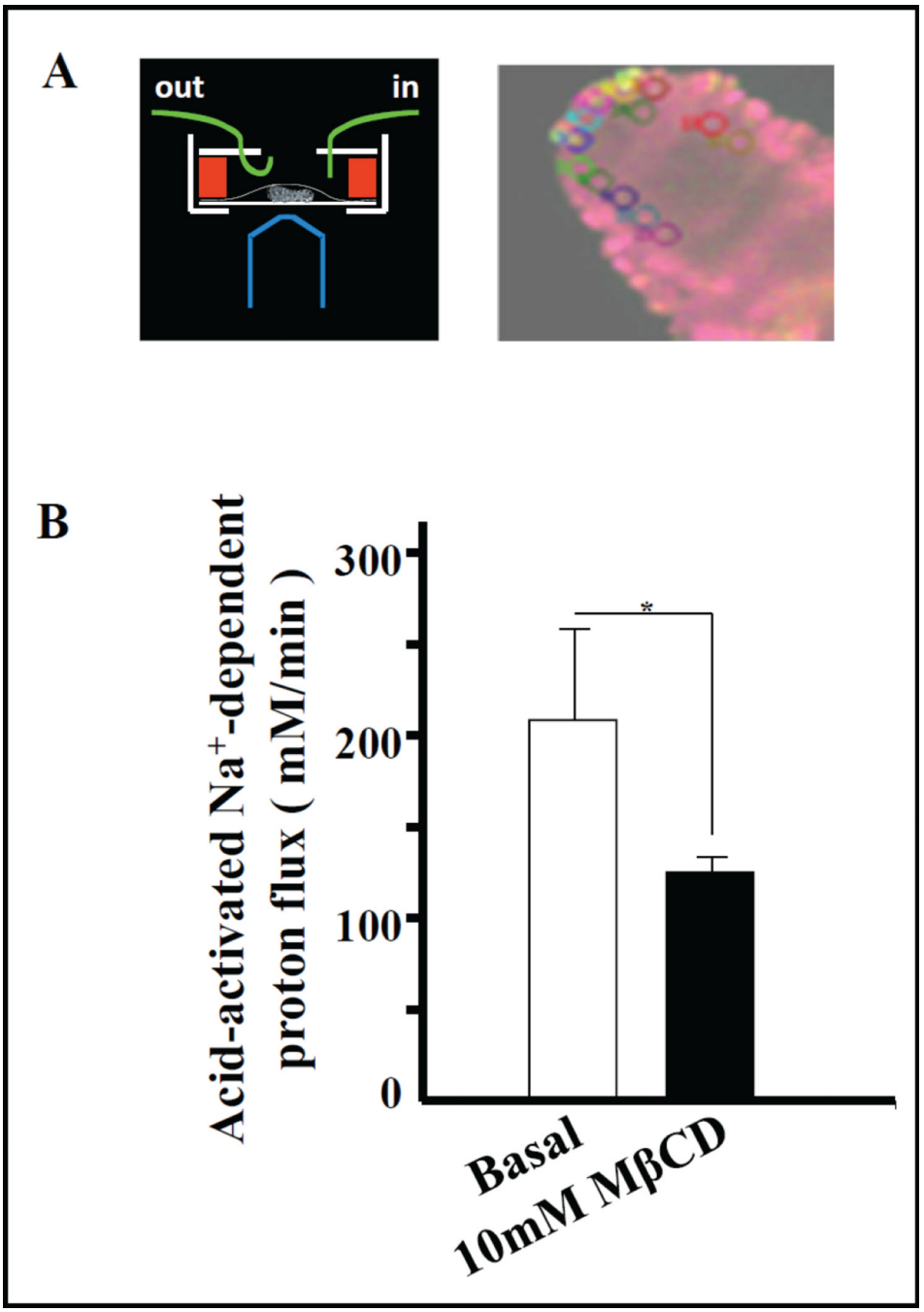

Fig. 5.

Modulation of NHE3 activity by cholesterol extraction. A) Schematic diagram of the villus perfusion chamber, and screenshot of BCECF-loaded villus with areas of interest (ROI) outlined. The villus has changed its dimension since placement of the ROIs, and the stored images of each experiment are rerun and the ROIs retraced after its completion. Pseudocolours indicate the 490/440 ratio. B) The activity of NHE3 in membrane rafts was estimated by measuring acid-activated Na^+-dependent proton flux (mM/min) before and

after disruption of rafts using 10mM MβCD superfusion for 10 min. NHE3 activity was reduced by ~22% after MβCD treatment. n=4 ($p<0.05$).

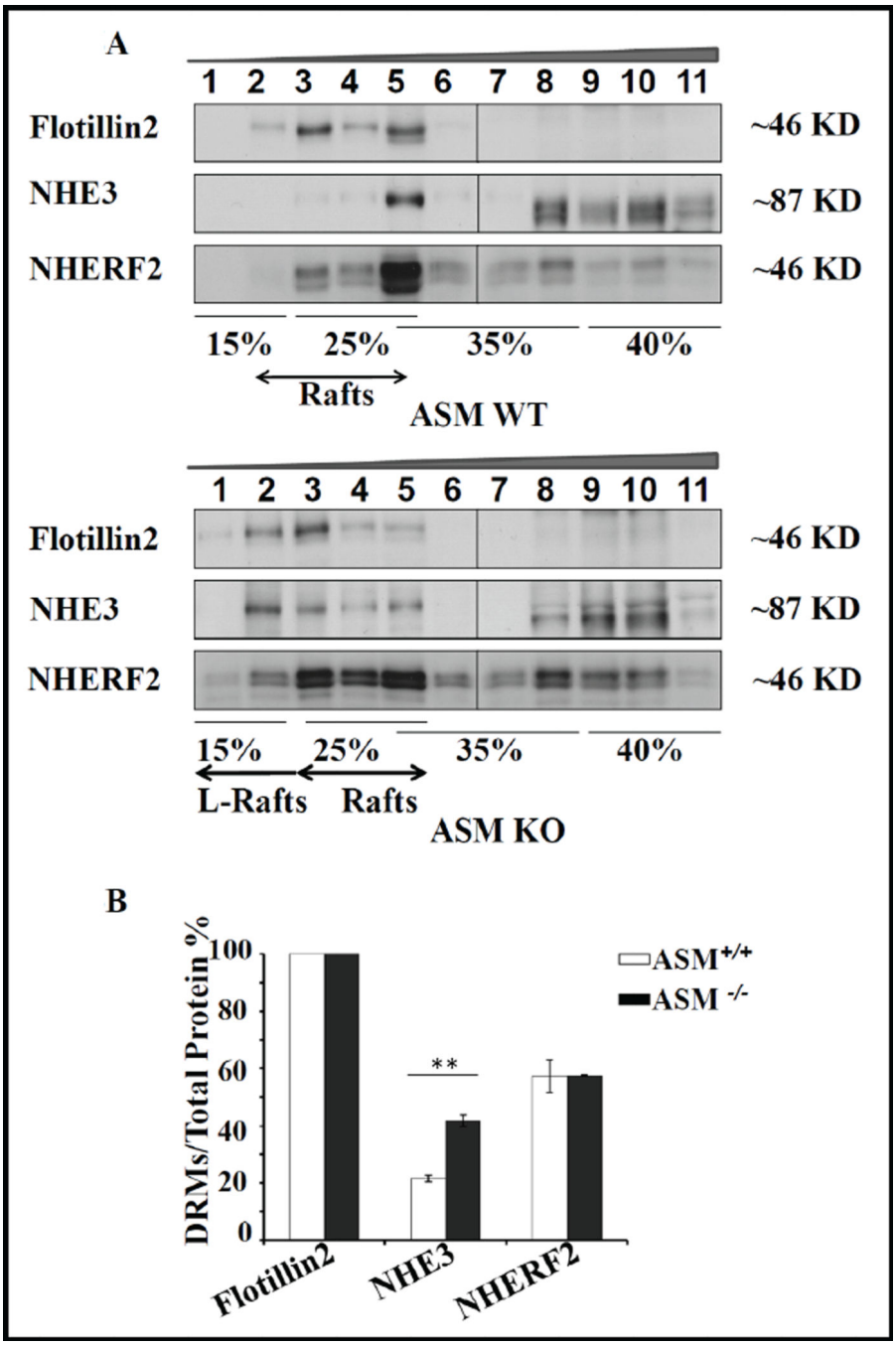

Fig. 6.

Membrane raft association of NHE3 and NHERFs is altered by a change in lipid composition of BBM. A) In the ASM KO mice, NHE3 was distributed into rafts and non-rafts, but there was a pronounced shift of both flotillin2 and NHE3 towards even lighter density OptiPrep fractions which we denote as “lighter rafts” (L-rafts). B) Quantitative analysis showed that there was a twofold increase in NHE3 pool in rafts in ASM KO, 50% of which was localized in L-rafts ($p<0.05$). n=3.

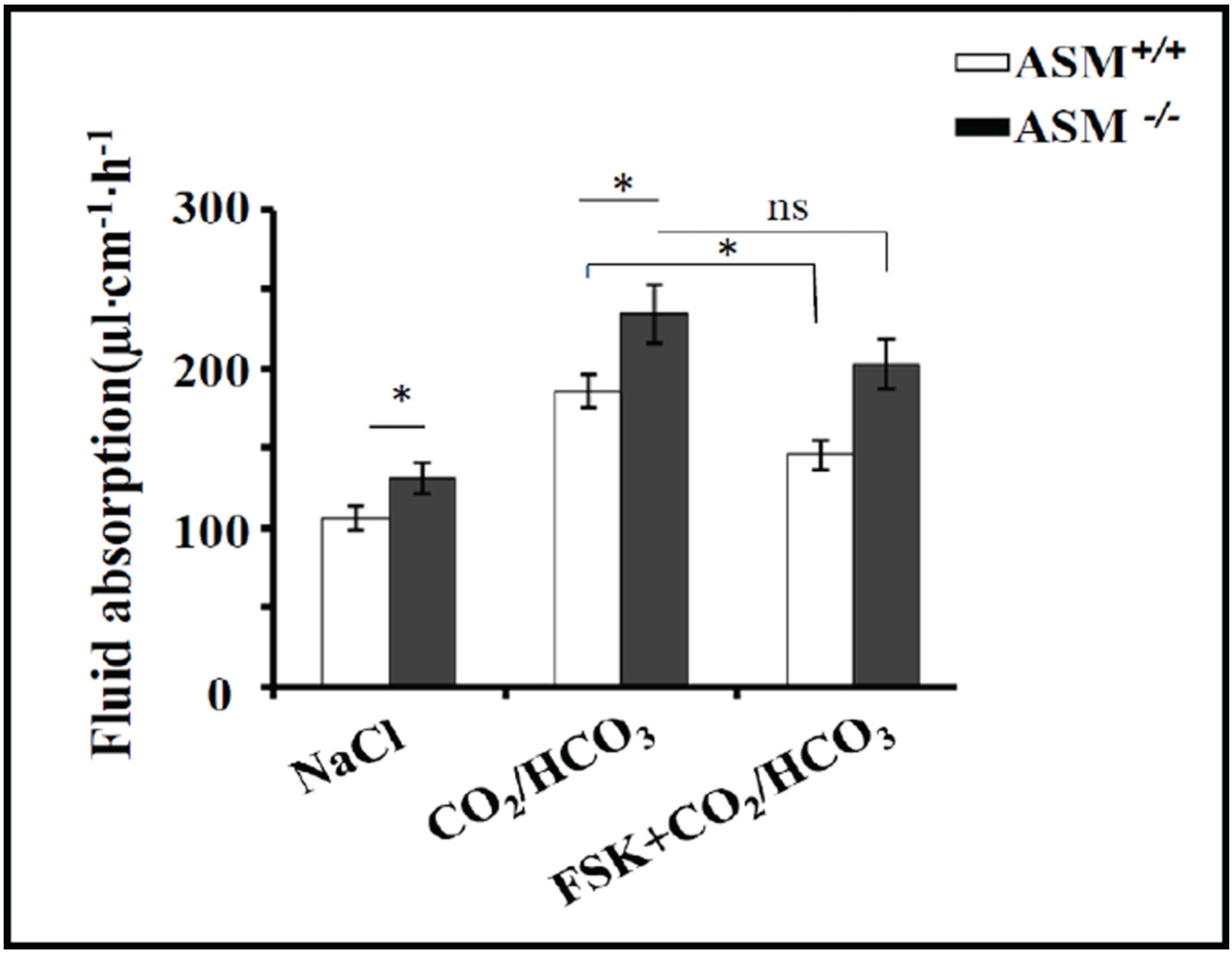

Fig. 7.

Modulation of sphingolipid composition of BBM alters small intestinal fluid absorptive rates. Basal fluid absorption *in vivo* (~60% mediated by NHE3), and CO_2/HCO_3^--stimulated fluid absorption (the stimulation being ~100% NHE3-dependent) were significantly higher in ASM KO than WT jejunum, while decrease in fluid absorption by 10 µM forskolin treatment only reached the level of significance in WT jejunum. WT n=10 and ASM KO n=9, ($p<0.05$).

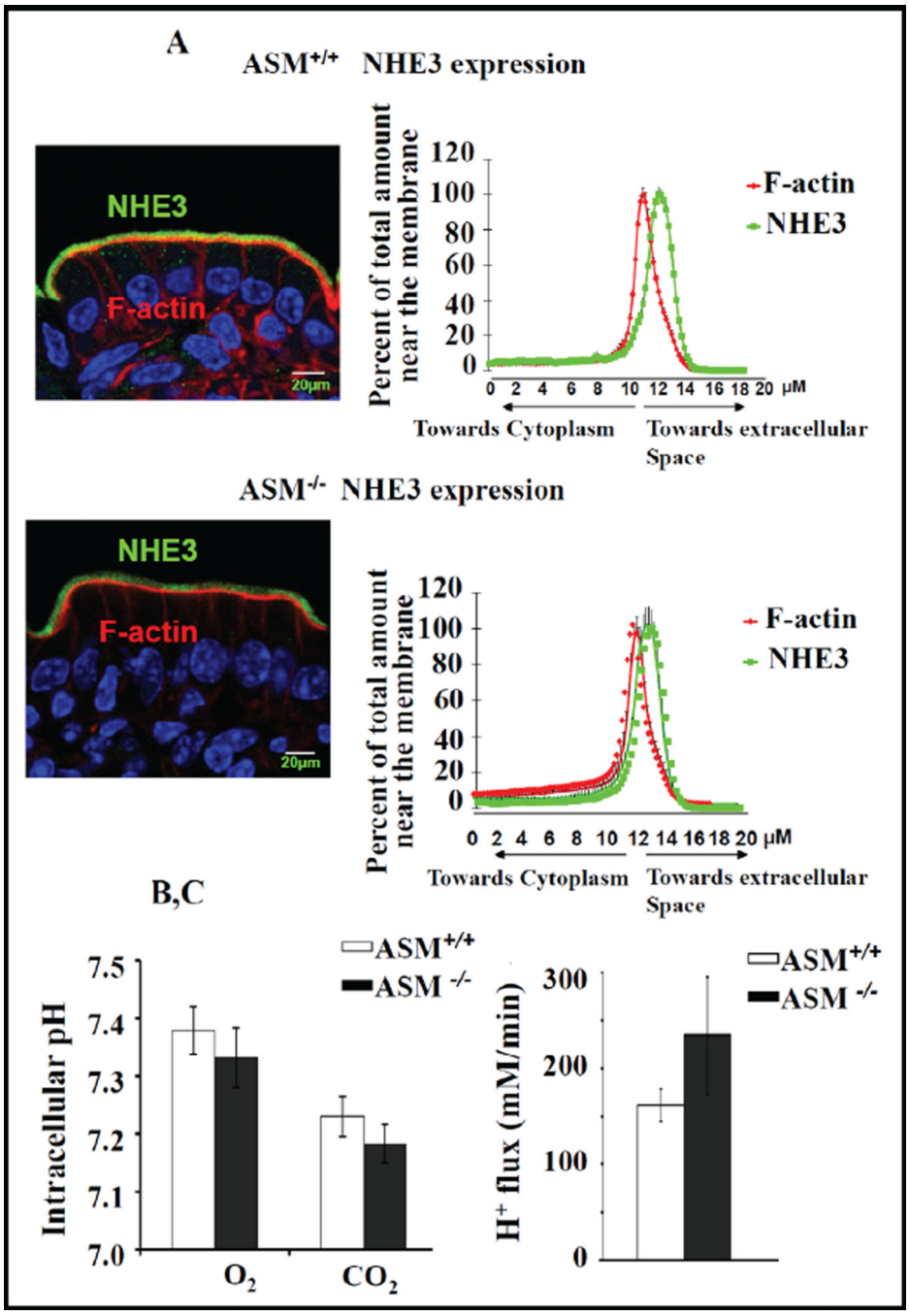

Fig. 8.

NHE3 BBM localization and acid-activated NHE3 activity was unaltered in ASM KO jejunum. A) NHE3 distribution along the terminal web-microvillar axis was similar in ASM KO and WT jejunal BBM. F-actin (red) was stained by phalloidin, NHE3 (green) by antibody staining, and the relative intensity distribution along the microvillar axis was analysed as described in the method section. The peak of Factin intensity denotes the terminal web/microvillar cleft region, and the majority of NHE3 was localized to the microvillar region (more toward the lumen) in ASM KO as well as WT jejunum. B) The

steady state pH_i, assessed fluorometrically in the enterocytes of jejunal villi from ASM WT and KO mice, was not significantly different. WT n=11 and ASM KO n=10 ($p<0.05$). C) The acid-activated NHE3 transport rate (which will measure the total membrane-resident NHE3 pool) was also similar for WT and ASM KO mice. WT n=16 and ASM KO n=12 ($p<0.05$).